

## The Turbulent Alfvénic Aurora

C. C. Chaston,<sup>1</sup> C. Salem,<sup>1</sup> J. W. Bonnell,<sup>1</sup> C. W. Carlson,<sup>1</sup> R. E. Ergun,<sup>2</sup> R. J. Strangeway,<sup>3</sup> and J. P. McFadden<sup>1</sup>

<sup>1</sup>Space Science Laboratory, University of California, Berkeley, California 94720, USA

<sup>2</sup>Laboratory for Atmospheric and Space Physics, University of Colorado, Boulder, Colorado 80303, USA

<sup>3</sup>Institute for Geophysical and Planetary Physics, University of California, Los Angeles, California 90095, USA

(Received 11 February 2008; published 30 April 2008)

It is demonstrated from observations that the Alfvénic aurora may be powered by a turbulent cascade transverse to the geomagnetic field from large MHD scales to small Alfvén wave scales of several electron skin depths and less. We show that the energy transport through the cascade is sufficient to drive the observed acceleration of electrons from near-Earth space to form the aurora. We find that regions of Alfvén wave dissipation, and particle acceleration, are localized or intermittent and embedded within a near-homogeneous background of large-scale MHD structures.

DOI: 10.1103/PhysRevLett.100.175003

PACS numbers: 94.30.Aa, 94.05.Lk, 94.05.Pt, 94.30.Tz

Recent observations have demonstrated that auroral electron acceleration occurs not only via the closure of large-scale geomagnetic field-aligned currents in the ionosphere but also through the action of small-scale Alfvén waves [1]. Figure 1 presents observations from NASA's FAST [2] spacecraft above the auroral oval along a trajectory through an aurora imaged in UV light [Fig. 1(a)] from the Polar spacecraft [3]. Figure 1(b) shows the electric ( $E_x$ ) and magnetic field ( $B_y$ ) measured through this aurora in a coordinate system where the  $x$  and  $y$  directions point nearly along and perpendicular to the FAST spacecraft trajectory, respectively, with both orthogonal to the local geomagnetic field ( $B_o$ ). From Ampere's law these observations can be ordered using the sign of the gradient in  $B_y$  as upward (yellow) and downward geomagnetic field-aligned currents (blue) and regions of fluctuating or filamentary current structure (green). It has previously been demonstrated that the regions of fluctuating current shown in green are dominated by interactions in Alfvén waves [4]. These regions of "Alfvénic aurora" are generally represented in spacecraft plasma measurements by electron energy flux spectrograms flat with energy up to a few keV and intense fluxes of accelerated ionospheric ions with energies extending up to a few 100 eV as represented in Figs. 1(c) and 1(d), respectively.

Particle acceleration in the Alfvénic aurora drives a significant fraction of auroral luminosity [5,6]. However, for observed wave and plasma properties small-scale Alfvén waves are so strongly damped that their observation at large distances from their source should be rare [7,8]. Consequently, a mechanism whereby wave energy at small scales is constantly replenished along geomagnetic field lines is required to account for observations. Models proposed to address this include phase mixing on transverse Alfvén speed gradients [9,10], feedback from the ionosphere [11–13], and various local instabilities [8,13–15]. In this Letter we show that this energy transfer may occur as a turbulent cascade composed of large-scale MHD structures and Alfvén waves on small scales transverse to

the geomagnetic field of the order of  $2\pi\lambda_e$  ( $\sim 2\pi \times 330$  m) and less. Here  $\lambda_e$  is the electron skin depth. These scales project to widths of the order of 1 km at an altitude of 100 km where ionization of the atmosphere by electrons accelerated in these waves provides the auroral

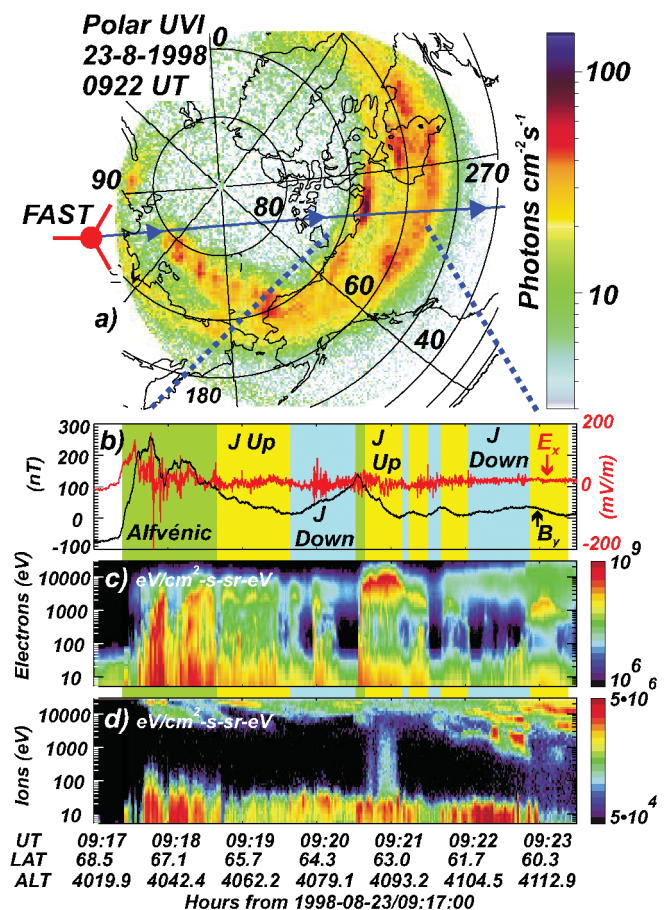


FIG. 1 (color). (a) UV auroral image from Polar UVI instrument and FAST spacecraft trajectory. (b) FAST  $E_x$  (red) and  $B_y$  (black) fields as defined in the text. (c),(d) FAST electron and ion spectrograms.

light seen from the ground. While turbulent cascades have long been studied in the solar wind [16] and more recently in Earth's magnetosheath [17] and plasma sheet [18], our results reveal the operation of such a cascade above the auroral oval.

Figure 2 shows averaged spectral results in  $B_y$  and  $E_x$  compiled from observations recorded from August 6 to September 9, 1998 from FAST at an altitude of  $\sim 4000$  km through the Alfvénic aurora above the night-side auroral oval near local midnight. In Fig. 2(a) the spectrogram for  $B_y$  is expressed as a function of wave frequency in the spacecraft frame ( $f_{sp}$ ), and, in the inset, wave number ( $k_x$ ) measured via interferometry. Interferometric measurement of the wave field is made possible by multipoint electric field measurements in the spacecraft spin plane [19,20]. The  $k$  spectra in  $B_y$  is then constructed under the assumption that at a given spacecraft frame frequency the  $k_x$  measurement applies to both field quantities. Comparison

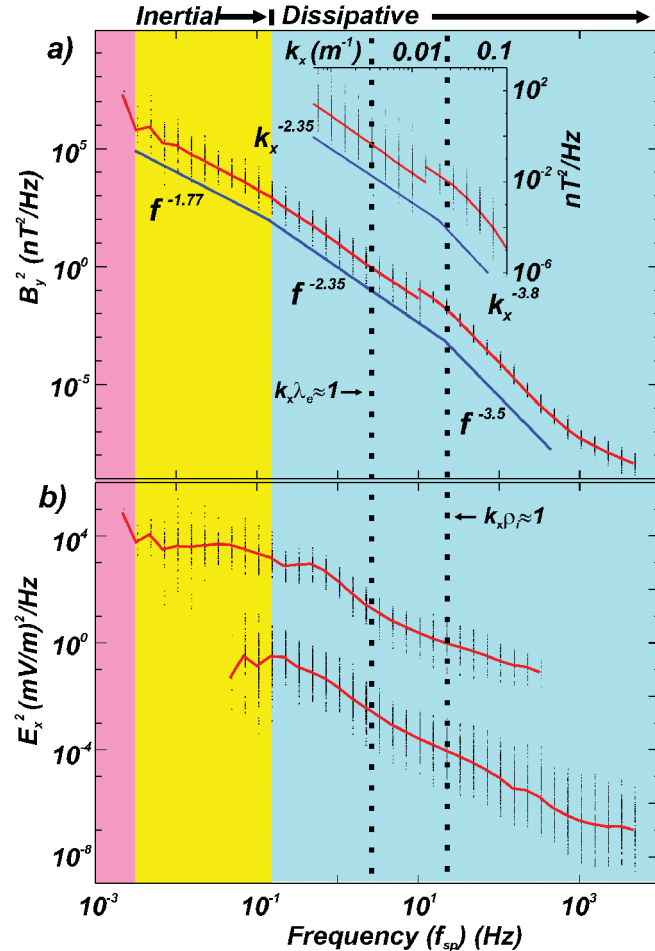


FIG. 2 (color). (a) Average  $B_y^2(f_{sp}, k_x)$  spectra. (b) Average  $E_x^2(f_{sp})$  spectra for survey and burst data collection modes. The latter is down-shifted by 4 orders of magnitude. The black bars are composed of points representing individual measurements in each  $f_{sp}$  or  $k_x$  bin.

of the spectral results in  $f_{sp}$  and  $k_x$  reveals that they are related through spacecraft Doppler shift as  $2\pi f_{sp} \approx k_x v_{sp}$  where  $v_{sp}$  is the spacecraft speed ( $\sim 5$  km/s) transverse to the geomagnetic field. For those variations at wave numbers smaller than those measurable from interferometry,  $2\pi f_{sp} \approx k_x v_{sp}$  remains valid and is commonly used in auroral science on these scales to determine field-aligned current strengths [21]. Consequently, to within the error of the spectral estimates, the scaling laws in  $f_{sp}$  and  $k_x$  over the ranges shown are approximately the same.

The spectral trends shown in Fig. 2(a) have features generally found in fluid turbulence [22] and turbulence in the solar wind [16]. With  $f_{sp}$  and  $k_x$  related through spacecraft Doppler shift we find for  $f_{sp} < 0.15$  Hz or  $k_x < 0.1/\lambda_e$  that  $B_y^2(k_x)$  varies as  $k_x^{-1.77 \pm 0.3}$  where the error defines the range of indices observed for all auroral traversals surveyed. We note that to within experimental uncertainty this dependency is equivalent to a Kolmogorov [22] scaling law ( $k_x^{-5/3}$ ) and predictions for strongly magnetized anisotropic incompressible MHD turbulence [23]. Over the next two decades in  $f_{sp}$  or  $k_x$  we find a  $k_x^{-2.35 \pm 0.2}$  ( $\sim k_x^{-7/3}$ ) law applies. This is similar to that found for kinetic Alfvén waves and mirror mode waves in the solar wind [24,25] and magnetosheath [17], respectively. Beyond this range, and over the next decade, a steeper slope is observed with  $B_y^2(k_x) \propto k_x^{-3.5 \pm 0.2}$ . The break point in this case occurs at  $k_x \rho_i \approx 1$  where  $\rho_i$  is the ion gyroradius in the geomagnetic field. Here we have assumed  $T_i = 1$  eV for  $O^+$  ions, which dominate the plasma at this altitude, based on expected ionospheric temperatures and the energy required to balance gravitation and the upward force due to the ion's magnetic moment in the Earth's diverging magnetic field. Figure 2(b) shows spectral estimates in  $E_x$  from both the continuously sampled survey observations and high resolution burst intervals (down-shifted by 4 orders of magnitude). Overall, for  $k_x \geq 0.1/\lambda_e$ ,  $E_x^2(k_x)$  varies as  $\sim k_x^{-1.7}$  similar to a previous case study [20]. However, in these statistical results, a power-law constant over more than a decade in  $k_x$  or  $f_{sp}$  is not clear.

Figure 3 shows the observed averaged  $E_x/B_y$  ratio for these wave fields and that expected from local Alfvén wave dispersion. For  $k_x \geq 3.0 \times 10^{-4} \text{ m}^{-1}$  ( $k_x \geq 0.1/\lambda_e$ ) the wave field statistics obey the local model in agreement with previous case studies [26,27]. Over this wave number range these waves are described as inertial Alfvén waves [28] and carry an electric field aligned with the geomagnetic field ( $E_z$ ) which can drive geomagnetic field-aligned electron acceleration through Landau damping [7,8]. The resulting dissipation of wave energy over this range in  $k_x$  will power the aurora [28] with widths mapped to 100 km altitude of  $\sim 10$  km and less. Conversely, at wave numbers  $k_x < 3.0 \times 10^{-4} \text{ m}^{-1}$  ( $k_x < 0.1/\lambda_e$ ), the observations deviate from that expected for the local dispersion of Alfvén

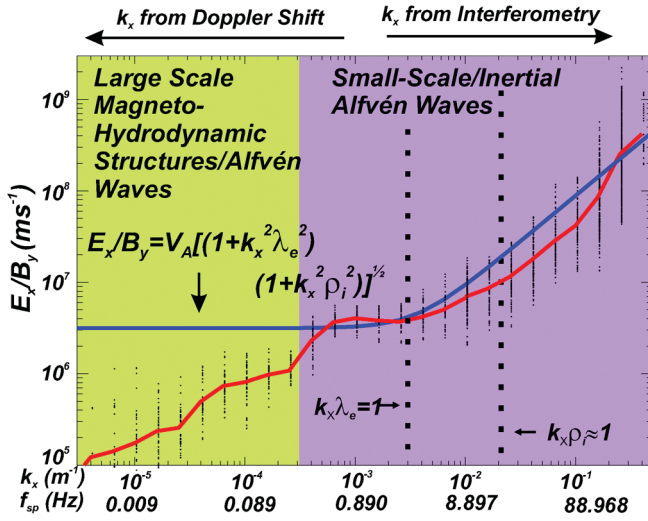


FIG. 3 (color). Observed average  $E_x/B_y(f_{sp}, k_x)$  ratio (red line). The blue line shows the predicted ratio given by local inertial Alfvén wave dispersion.

waves. These waves or structures occur on scales that are comparable to the distances over which the plasma parameters along the geomagnetic field vary and so have characteristics not well described by local wave dispersion. These waves or structures provide no measurable field compression and do not provide an  $E_z$ . Together with the Kolmogorov-like spectral scaling shown in Fig. 2, these observations suggest that fluctuations over this range in  $k_x$  may constitute what is known in turbulence phenomenology as an inertial subrange [22].

Further insight into the nature of the turbulent fluctuations observed is provided by the probability density functions (PDFs) [16] given by  $\delta B_y(\delta x) = B_y(x + \delta x) - B_y(x)$  and shown in Fig. 4(a).  $\delta x \approx v_{sp} \Delta t$  represents a spatial step along the spacecraft trajectory, or in this case through Doppler shift, equivalently a time step ( $\Delta t$ ). For each  $\delta x$  considered,  $\delta B_y$  is binned in standard deviations ( $\sigma$ ) from the mean with a bin width of  $\Delta \sigma = 0.2\sigma$ . These PDFs have also been normalized by  $\Delta \sigma N$  where  $N$  is the total number of differences taken. To quantify the intermittency of the fluctuations observed we fit a Castaing distribution [29] [shown by the dotted lines in Fig. 4(a)] to each PDF where the deviation from a Gaussian PDF of fluctuation amplitudes with increasing intermittency is represented by increases in the parameter  $\lambda_c$  from a value of zero. Figure 4(a) shows that for the largest  $\delta x$  the PDF is close to Gaussian in form with  $\lambda_c \rightarrow 0$ . However, for  $\delta x/(2\pi\lambda_e) \rightarrow 1$  we find a roughly exponential dependence of the PDF on  $\sigma$  and for the smallest scales considered we find that the wings of the distribution are curved outwards with  $\lambda_c \rightarrow 1$  representing intermittency.

Taking the moments of these PDFs we obtain the structure functions [16] defined as  $S_p(\delta x) = \langle |\delta B_y(\delta x)|^p \rangle$  and presented in Fig. 4(b). The first two scale-invariant ranges

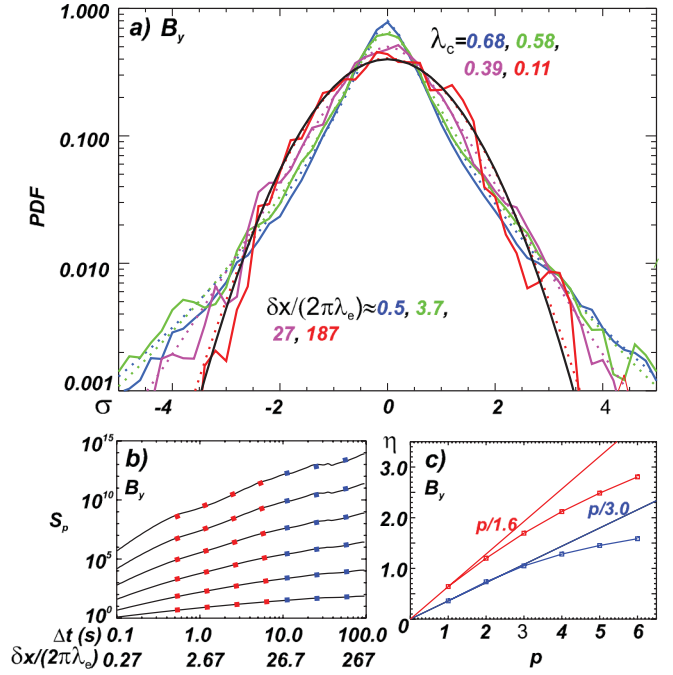


FIG. 4 (color). (a) Normalized PDFs. Solid lines show observations, dotted lines are fits of the Castaing model. (b) Structure functions based on PDFs in (a). The blue and red dotted lines correspond to fits of  $S_p \propto \delta x^{\eta(p)}$ . (c) The scaling exponent  $\eta$  derived from the fits shown in (b).

suggested from the spectral plot of Fig. 2(a) can be identified as the linear portions overplotted by  $S_p \propto \delta x^{\eta(p)}$  shown by the blue and red dashed lines. The scaling exponent  $\eta$  derived from these fits is shown in Fig. 4(c). In the case of the larger scale range (blue) we find that for  $p = 1-3$  the magnetic field approximately obeys the expected trend for homogeneous Kolmogorov turbulence with  $\eta(p) \approx p/3$ . This result provides evidence for the existence of an inertial subrange over this range of scales (i.e.,  $k_x < 3.0 \times 10^{-4} \text{ m}^{-1}$  or  $k_x < 0.1/\lambda_e$ ). For the smaller scale range (red) the scaling exponent has generally convex form in  $p$ , suggesting a multifractal scaling of the field variations. Physically this is indicative of turbulence where the occupancy of space by the turbulent fields varies along the spacecraft trajectory and across scales suggestive of a stretching of eddies into filamentary vortices. These observations together with those shown in Figs. 2 and 3 provide statistical evidence for the existence above the auroral oval of a Kolmogorov-like background of near-homogeneous MHD turbulence on large scales in which more localized or intermittent regions of dissipation are embedded.

Since the inertial subrange spectra and structure functions are consistent with the Kolmogorov model [22] we invoke Kolmogorov's 1941 two-thirds law to determine if the energy transport rate through the cascade is sufficient to power the electron acceleration observed. We note that this

is identical to that derived for anisotropic incompressible MHD turbulence in a strongly magnetized plasma [23] as we observe. Formulated in terms of the magnetic field energy spectrum this is given by [24]

$$\varepsilon = \frac{2\pi}{v_{sp}} \left( \frac{3}{5} \alpha \right)^{-3/2} [F(f_{sp})]^{3/2} f_{sp}^{5/2}, \quad (1)$$

where  $\varepsilon$  is the energy transport rate in  $\text{J kg}^{-1} \text{s}^{-1}$  through the cascade. For large Reynolds number [30]  $\alpha \approx 1.5$  and  $F(f_{sp}) = B_y(f_{sp})^2 / (2\mu_o \rho)$  where  $\rho$  is the mass density. Averaging this expression over the inertial subrange identified in Fig. 2 we find that the energy transport rate through the cascade is  $\varepsilon_{\text{FAST}} \approx 2.5 \times 10^7 \text{ J kg}^{-1} \text{ s}^{-1}$  or in spatial units  $2.5 \times 10^{-10} \text{ W/m}^3$ . From conservation of energy and the guidance of Alfvén waves and electrons along the geomagnetic field, it can be shown that the change in down-going electron energy flux at the FAST satellite due to electron acceleration in the turbulent wave fields over a distance  $\Delta z$  along the geomagnetic field above FAST is  $\Delta \xi_{\text{FAST}} \leq \varepsilon_{\text{FAST}} \Delta z$ . Averaging electron measurements over the same intervals for which the spectral data were collected we find  $\xi_{\text{FAST}} = 1.6 \text{ mW/m}^2$ . Consequently, to account for  $\xi_{\text{FAST}}$  requires  $\Delta z \geq 6000 \text{ km}$ . This result is consistent with observations and simulations of the electron acceleration process in Alfvén waves above the aurora which has been demonstrated to occur over a distance along geomagnetic field lines of a few Earth radii [4,7,31]. These statistical results then demonstrate that the Alfvénic aurora may be driven by the transport of energy through a turbulent cascade from large nondissipative MHD scales to kinetic Alfvén waves scales ( $\leq 2\pi\lambda_e$ ) where electron acceleration and wave dissipation are observed to proceed.

These observations provide a statistical argument that the Alfvén wave driven aurora may be powered via a turbulent cascade. The scaling law we observe in the inertial range is consistent with the predictions of Goldreich and Sridhar [23] for anisotropic Kolmogorov-like incompressible MHD turbulence where energy flux is directed through the cascade to larger  $k_x$ . The cascade is facilitated by the interaction of counterpropagating Alfvén waves which are naturally provided in the auroral context through wave reflection from the ionosphere [13]. Dissipation occurs through field-aligned electron acceleration for  $k_x \lambda_e > 0.1$  for which the wave carries a significant  $E_z$ . The second spectral break point at  $k_x \rho_i \approx 1$  suggests ion acceleration also contributes to dissipation. Measurements of the bursty or intermittent nature of these field fluctuations show the existence of a near-homogeneous background of nondissipative MHD structures in which localized regions of dissipation and particle acceleration are embedded. Observations at altitudes above the FAST spacecraft [31] suggest that this cascade proceeds on geomagnetic field lines extending from the source regions of the large-scale fluctuations in the outer magnetosphere to the auroral ionosphere. These large-scale fluctuations in-

ject energy into the cascade which is transported to smaller scales along geomagnetic field lines to drive electron acceleration and ultimately power the Alfvénic aurora.

This research was supported by NASA Grants No. NNG06GG63G and No. NAG5-3596.

- 
- [1] G. Paschmann, S. Haaland, and R. Treumann, *Auroral Plasma Physics* (Kluwer Academic, Dordrecht, 2003), p. 94.
  - [2] R. Pfaff *et al.*, *Space Sci. Rev.* **98**, 1 (2001).
  - [3] M. Brittacher *et al.*, *Adv. Space Res.* **20**, 1037 (1997).
  - [4] C. C. Chaston *et al.*, *J. Geophys. Res.* **108**, 8003 (2003).
  - [5] A. Keiling *et al.*, *Science* **299**, 383 (2003).
  - [6] C. C. Chaston *et al.*, *Geophys. Res. Lett.* **34**, L07101 (2007).
  - [7] R. L. Lysak and W. Lotko, *J. Geophys. Res.* **101**, 5085 (1996).
  - [8] V. Genot, P. Louarn, and F. Mottez, *Ann. Geophys.* **22**, 2081 (2004).
  - [9] R. L. Lysak and Y. Song, in *Magnetospheric Current Systems*, edited by S. Ohtani *et al.* (AGU Geophysical Monograph, Washington, DC, 1999), p. 147.
  - [10] W. Allan and A. Wright, *J. Geophys. Res.* **105**, 317 (2000).
  - [11] R. L. Lysak, *J. Geophys. Res.* **96**, 1553 (1991).
  - [12] A. V. Streltsov and W. Lotko, *J. Geophys. Res.* **109**, A09214 (2004).
  - [13] C. E. Seyler, *J. Geophys. Res.* **95**, 17 199 (1990).
  - [14] J. Penano and G. Ganguli, *J. Geophys. Res.* **105**, 7441 (2000).
  - [15] N. Singh, G. Khazanov, and A. Mukhter, *J. Geophys. Res.* **112**, A06210 (2007).
  - [16] R. Bruno and V. Carbone, *Living Rev. Solar Phys.* **2**, 4 (2005).
  - [17] F. Sahraoui *et al.*, *Phys. Rev. Lett.* **96**, 075002 (2006).
  - [18] J. E. Borovsky and H. O. Funsten, *J. Geophys. Res.* **108**, 1284 (2003).
  - [19] J. W. Bonnell *et al.*, in *Proceedings of the American Geophysical Union, Fall Meeting 2001* (American Geophysical Union, Washington, DC, 2001), Abstract No. 2001AGUFMSM51B0823B.
  - [20] C. C. Chaston *et al.*, *J. Geophys. Res.* **111**, A03206 (2006).
  - [21] T. Iijima and T. Potemra, *Geophys. Res. Lett.* **9**, 442 (1982).
  - [22] A. N. Kolmogorov, *C.R. Acad. Sci. URSS* **32**, 16 (1941); reprinted in *Proc. R. Soc. A* **434**, 15 (1991).
  - [23] P. Goldreich and S. Sridhar, *Astrophys. J.* **438**, 763 (1995).
  - [24] R. J. Leamon *et al.*, *J. Geophys. Res.* **104**, 22 331 (1999).
  - [25] S. D. Bale *et al.*, *Phys. Rev. Lett.* **94**, 215002 (2005).
  - [26] J.-E. Wahlund *et al.*, *J. Geophys. Res.* **103**, 4343 (1998).
  - [27] K. Stasiewicz *et al.*, *Geophys. Res. Lett.* **27**, 173 (2000).
  - [28] C. K. Goertz and R. W. Boswell, *J. Geophys. Res.* **84**, 7239 (1979).
  - [29] B. Castaing, Y. Gagne, and E. J. Hopfinger, *Physica (Amsterdam)* **46D**, 177 (1990).
  - [30] L. D. Landau and E. M. Lifshitz, *Fluid Mechanics* (Pergamon, New York, 1959), 1st ed.
  - [31] J. R. Wygant *et al.*, *J. Geophys. Res.* **107**, 1201 (2002).